

Article

# Robustness of Optimal Sensor Methods in Dynamic Testing–Comparison and Implementation on a Footbridge

Marc Lizana \* and Joan R. Casas 

Department of Civil and Environmental Engineering, ETSCCPB, Universitat Politècnica de Catalunya, Carrer de Jordi Girona 1, 08034 Barcelona, Spain; joan.ramon.casas@upc.edu

\* Correspondence: marc.lizana@estudiantat.upc.edu

**Abstract:** One of the objectives of structural health monitoring (SHM) is to maximize the information while keeping the number of sensors, and consequently the cost of the sensor system, to a minimum. Besides, the sensor configurations must be robust in the sense that the feasibility of small errors inherent to the process must not lead to large variations in the final results. This paper presents novelties regarding the robustness evaluation to model and measurement errors of four of the most influential optimal sensor placement (OSP) methods: the modal kinetic energy (MKE) method; the effective independence (EFI) method; the information entropy index (IEI) method; and the MinMAC method. The four OSP methods were implemented on the Streicker Bridge, a footbridge located on the Princeton University Campus, to identify five mode shapes of the bridge. The mode shapes, obtained in a FE model's modal analysis, were used as input data for the OSP analyses. The study indicates that the MKE method seems to be the most suitable method to estimate the optimal sensor positions: it provides a relatively large amount of information with the lowest computational time, and it outperforms the other three methods in terms of robustness in the usual range of number of sensors.



**Citation:** Lizana, M.; Casas, J.R. Robustness of Optimal Sensor Methods in Dynamic Testing–Comparison and Implementation on a Footbridge. *Dynamics* **2022**, *2*, 149–160. <https://doi.org/10.3390/dynamics2020007>

Academic Editors: Cesare Biserni and Christos Volos

Received: 7 April 2022

Accepted: 1 June 2022

Published: 4 June 2022

**Publisher's Note:** MDPI stays neutral with regard to jurisdictional claims in published maps and institutional affiliations.



**Copyright:** © 2022 by the authors. Licensee MDPI, Basel, Switzerland. This article is an open access article distributed under the terms and conditions of the Creative Commons Attribution (CC BY) license (<https://creativecommons.org/licenses/by/4.0/>).

**Keywords:** optimal sensor placement; robustness evaluation; structural dynamics; dynamic testing; modal analysis; footbridge

## 1. Introduction

Structural health monitoring (SHM) is being widely used for the safety assessment and management of existing bridges and structures. SHM systems are expected to obtain the maximum amount of information from structural response. In general, the higher the number of sensors placed, the more detailed the information is on the structure.

One of the main challenges related to SHM is to optimize the trade-off between the maximal information obtained by the sensor system and the material costs for the experimental set-up. Cost-benefit analyses of SHM systems can be found in the literature (e.g., in [1] applied to structural damage of a bridge pier, in [2] applied to a tall building).

This paper investigates some of the most influential optimal sensor placement (OSP) methods and presents the implementation of the methods on a footbridge for the identification of the first five mode shapes. An evaluation of the OSP methods is performed for different numbers of target sensors in terms of robustness.

The sensor configurations must be robust to the existence of error effects in the process. There are two types of errors that cause inaccuracies in the estimates: the model error and the measurement error [3]. On the one hand, the model error occurs as inaccurate or oversimplified assumptions about the actual structure are used to construct a model of the structure, normally a numerical or finite element model. The model error leads to bias in the estimates, and many observations do not eliminate the bias. On the other hand, the measurement error is due to noise effects that contaminate the experimental data. This noise can be induced by electrical devices, problems with cables, etc. This type of error is defined as a random error and produces imprecise measurements, but not bias.

## 2. Optimal Sensor Placement Methods

In this section, four well-known and widely used optimal sensor placement (OSP) methods are investigated: the modal kinetic energy (MKE) method, the effective independence (EFI) method, the information entropy index (IEI) method and the MinMAC method. These four methods consider uniaxial sensors and are based on the optimization of different criteria (Yi and Li [4]): the measured energy per mode, the Fisher information matrix (FIM), the information entropy (IE) and modal assurance criterion (MAC).

Apart from the four presented methods, a lot of different methods can be used for the optimization of OSP problems such as deterministic optimization methods (e.g., Newton methods, linear/nonlinear programming) and combinatorial optimization methods (e.g., genetic algorithms, simulated annealing algorithm) [4].

### 2.1. Modal Kinetic Energy (MKE) Method

The modal kinetic energy (MKE) method (Krammer [5]), is related to the measured energy per mode criterion and formulates the kinetic energy distribution as follows:

$$MKE = \text{diag}(M\phi\phi^T) \quad (1)$$

For  $m$  target mode shapes and  $n$  degrees of freedom (DOFs),  $\phi$  is the  $[n \times m]$  mode shape matrix and  $M$  is the  $[n \times n]$  mass matrix. Therefore,  $MKE$  is a  $[n \times 1]$  vector with elements that correspond to the kinetic energy associated to each DOF considering multiple mode shapes.

The DOFs are ranked according to their kinetic energy value and the  $N_0$  DOFs with the highest values are retained as the optimal sensor locations, with  $N_0$  being the number of target sensors. The MKE method is not an iterative method.

### 2.2. Effective Independence (EFI) Method

The effective independence (EFI) method (Krammer [5]) is an iterative method based on the backward sequential sensor placement (BSSP) algorithm and the Fisher Information Matrix (FIM). The FIM is defined as follows:

$$Q(L) = (L\phi)^T(L\phi) \quad (2)$$

where,  $\phi$  is the matrix of mode shapes (dimensions  $[n \times n]$ , or  $[n \times m]$  if  $m$  target modes are considered),  $L$  is the Boolean  $[n \times n]$  matrix that maps the sensor locations to the  $n$  DOFs. Thus, the Fisher information matrix  $Q$  is a  $[n \times n]$  matrix, or a  $[m \times m]$  matrix if  $m$  target modes are considered.

A backward sequential sensor placement (BSSP) algorithm works as follows: it starts with all the DOFs of the structure monitored and sensors are removed, one by one, from the position that results in the smallest increase in the objective function. This procedure is continued up to the number of target sensors  $N_0$  is reached.

The EFI method aims to maximize the linear independence between the  $m$  target mode shapes throughout the following  $[n \times 1]$  vector:

$$E_D = [L\phi\psi] \circ [L\phi\psi] \text{diag}(\Lambda)^{-1} \quad (3)$$

where, the operator  $\circ$  denotes the Hadamard product (element-wise multiplication) and  $\Lambda$  and  $\psi$  are the  $[m \times m]$  matrices of eigenvalues and eigenvectors, respectively, of the following eigenvalue problem:

$$Q(L)\psi = \psi\Lambda \quad (4)$$

$\mathbf{Q}$  is the  $[m \times m]$  Fisher Information Matrix (FIM) defined in Equation (2). According to Krammer [5], the independence distribution vector  $\mathbf{E}_D$ , defined in Equation (3), can be alternatively formulated as follows:

$$\mathbf{E}_D = \text{diag} \left( (\mathbf{L}\boldsymbol{\phi}) \left[ (\mathbf{L}\boldsymbol{\phi})^T (\mathbf{L}\boldsymbol{\phi}) \right]^{-1} (\mathbf{L}\boldsymbol{\phi})^T \right) \quad (5)$$

where the procedure starts with all the DOFs instrumented. Therefore,  $\mathbf{L}$  equals to the identity matrix as before applying the method, in every iteration, the DOF with the lowest value in vector  $\mathbf{E}_D$  is removed from the sensor set and the mapping matrix  $\mathbf{L}$  is updated. The procedure is continued up to the number of target sensors  $N_0$  is reached.

### 2.3. Information Entropy Index (IEI) Method

The information entropy index (IEI) method, adopted by Papadimitriou and Lombaert [6], is an iterative method, which aims to find a sensor set that minimizes the information entropy (IE). The information entropy (IE) is the measure of uncertainty contained in the system parameters  $\boldsymbol{\theta}$  and it is defined as follows:

$$IE(\mathbf{L}, \boldsymbol{\theta}_0) = \frac{1}{2} N_\theta \ln(2\pi) - \frac{1}{2} \ln[\det\{\mathbf{Q}(\mathbf{L}, \boldsymbol{\theta}_0)\}] \quad (6)$$

where,  $\boldsymbol{\theta}_0$  is the optimal value of the parameter set  $\boldsymbol{\theta}$  of length  $N_\theta$  (number of parameters) that minimizes the IE, and  $\mathbf{Q}(\mathbf{L}, \boldsymbol{\theta}_0)$  is the  $[N_\theta \times N_\theta]$  FIM. For the case of modal identification, the parameters that are of interest are the modal coordinates. Hence, the parameter set  $\boldsymbol{\theta}$  becomes a  $[m \times 1]$  vector for  $m$  target modes and  $\mathbf{Q}(\mathbf{L}, \boldsymbol{\theta}_0)$  becomes a  $[m \times m]$  matrix.

The information entropy index (IEI), defined in Equation (7), is a normalized version of the information entropy [6].

$$IEI(\mathbf{L}, \boldsymbol{\theta}_0) = \sqrt{\frac{\det\mathbf{Q}(\mathbf{L}_{ref}, \boldsymbol{\theta}_0)}{\det\mathbf{Q}(\mathbf{L}, \boldsymbol{\theta}_0)}} \quad (7)$$

where,  $\boldsymbol{\theta}_0$  is the optimal value of the parameters set  $\boldsymbol{\theta}$  of length  $N_\theta$  (number of parameters), and  $\mathbf{Q}(\mathbf{L}, \boldsymbol{\theta}_0)$  is the  $[N_\theta \times N_\theta]$  FIM.  $\mathbf{L}_{ref}$  is the reference sensor configuration matrix, which is equal to the identity matrix if all the DOFs are monitored.

The IEI method can be used in combination with the backward sequential sensor placement (BSSP) algorithm: initially, the full configuration ( $n$  DOFs monitored) is assumed as a reference and then it is compared to all the possible configurations with one sensor less ( $n - 1$ ). The configuration with the lowest IEI is chosen and used in the following iteration. The procedure is continued up to the number of target sensors  $N_0$  is reached.

### 2.4. MinMAC Method

The MinMAC method (Carne and Dohrmann [7]), is an iterative method based on the forward sequential sensor placement (FSSP) algorithm and the modal assurance criterion (MAC).

The MAC index is an indicator of the degree of correlation between two mode shapes. The function of MAC index is to provide a measure of consistency (degree of linearity) between estimates of a modal vector. Usually, the MAC index is used to compare an experimental mode shape with a numerical mode shape. Nevertheless, mode shapes from two finite element (FE) models and from the same FE model (self-MAC) can be also compared.

The MAC index for a couple of  $[n \times 1]$  column vectors  $\phi_i$  and  $\phi_j$  of the mode shape matrix of a structure is defined as a scalar constant relating to the degree of consistency (linearity) between one modal vector and another reference modal vector:

$$MAC_{ij} = \frac{(\phi_i^T \phi_j)^2}{(\phi_i^T \phi_i)(\phi_j^T \phi_j)} \quad (8)$$

The MAC is a value that ranges between zero and one: a high value indicates a strong correlation between the two modes in comparison, while a low value indicates that the correlation is weak. MAC values can be represented in a MAC matrix. In the MAC matrix, diagonal elements are expected to be close to one whereas off-diagonal elements are expected to be close to zero.

The basic steps of the forward sequential sensor placement (FSSP) algorithm are: being  $N_0$  the number of target sensors, the position of the first sensor is chosen as the one that gives the highest reduction in the objective function. Similarly, the second sensor is in the position that gives the highest reduction in the objective function by assuming that the first sensor was already located at its optimal position. This procedure is continued up to the number of target sensors  $N_0$  is reached.

The MinMAC method consists of minimizing the maximum of the off-diagonal terms (MOD) of the MAC matrix (see Equation (8)) in order to determine an optimal sensor set. The basic steps of the MinMAC method are the following:

1. Choose  $N$  sensor locations (less than the required number of sensors  $N_0$ ) on intuition based on a visual inspection of the structure response;
2. The self-MAC matrix of the FEM modes is calculated for the initial sensor configuration plus one sensor ( $N+1$ ). The diagonal elements of the self-MAC matrices are unity, in contrast to a cross-MAC matrix between FEM modes and test modes [7]. The configuration that minimizes the MOD is chosen and used in the following iteration;
3. The procedure is continued up to the number of target sensors  $N_0$  is reached.

As an alternative to the intuition set, an initial sensor configuration can be selected using another OSP method (e.g., the EFI method).

### 3. Description of the Footbridge and FE Model

#### 3.1. Description of the Footbridge

The Streicker Bridge is a footbridge located on the Princeton University Campus (Princeton, New Jersey, USA). This bridge was chosen to test different optimal sensor placement (OSP) methods as it is instrumented with two fiber-optic-based monitoring systems: a discrete fiber Bragg-grating (FBG) monitoring system and a distributed sensing using Brillouin optical time domain analysis (BOTDA) monitoring system. The footbridge is 104 m long and consists of a main span and four legs (see Figure 1).

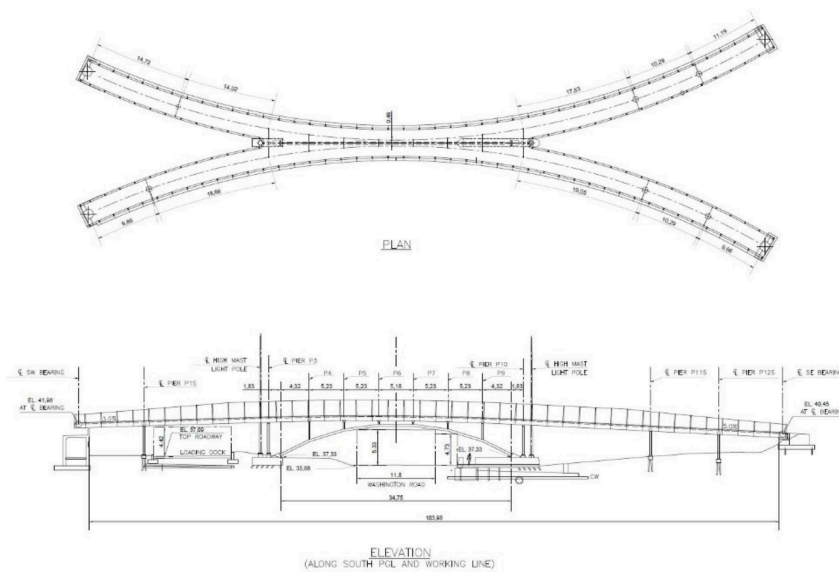


**Figure 1.** Plan and elevation drawings of the Streicker Bridge (PU and HNTB) [8].

The deck is made of post-tensioned high-performance concrete. The deck is connected through six spandrels to a steel arch in the main span (deck-stiffened arch) and is supported by eight Y-shaped piers in the lateral legs (see Figure 2). Arch, spandrels and piers are made of weathering steel tubes filled with self-consolidating concrete.

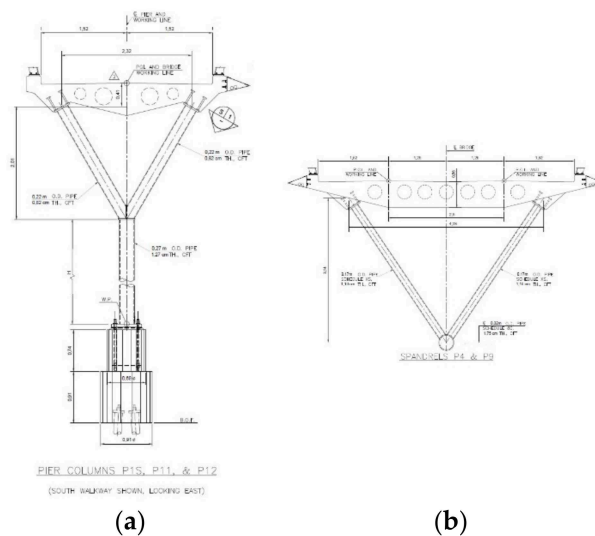


**Figure 2.** (a) Detail of one pier; (b) Detail of spandrel (PU & HNTB) [8].

Both piers and arch are supported on concrete footings. The deck is connected to piers and spandrels through fixed connections. At the four abutments, the deck rests on elastomeric neoprene bearings.

### 3.2. FE Model of the Footbridge

A three-dimensional finite element (FE) model of the footbridge built by Lizana [8] (see Figure 3) was used to provide input data for the OSP methods. The FE model, built in ANSYS Mechanical APDL, contains 97 nodes and 83 Timoshenko beam elements with six DOFs at each node.

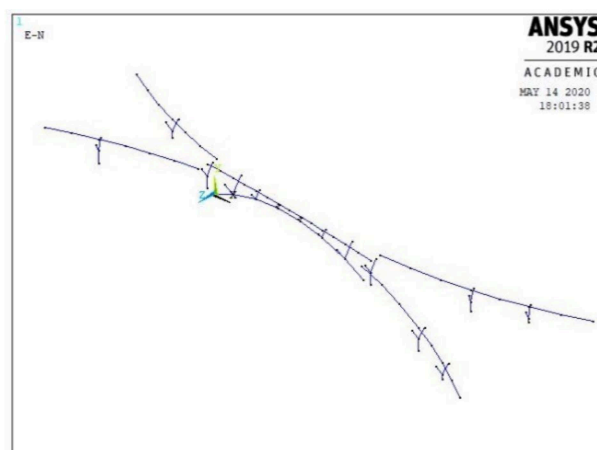


**Figure 3.** View of FE model in ANSYS [8].

The deck is connected to piers and spandrels through rigid body constraints that link the centroid of the deck to the two upper nodes of every Y-shaped pier and spandrel and constrain the six DOFs. Based on the structural drawings of the bridge, the bases of the piers and of the arch are fixed supports in the FE model, while the supports at the four abutments are hinged supports where all translations are constrained.

### 3.3. Modal Frequencies of the Footbridge

The first five eigenmodes, reported in Table 1, were used as input to the OSP analysis ( $m = 5$ ). The mode shapes related to the first five eigenmodes can be considered flexural (vertical displacements are dominant) according to the modal deformations in the FE model and the modal participation mass.

**Table 1.** Modal frequencies calculated using FE model [8].

Mode N.	Mode Shape	$f_{FEM}$ (Hz)
1	Flexural	3.12
2	Flexural	3.22
3	Flexural	3.60
4	Flexural	3.76
5	Flexural	4.19

## 4. Robustness Evaluation of the OSP Methods

In this section, a robustness evaluation of the OSP methods is presented. The sensor configurations must be robust to the existence of error effects in the process. There are two types of errors that cause inaccuracies in the estimates: the model error and the measurement error [3].

On the one hand, the model error occurs due to inaccurate or oversimplified assumptions about the actual structure being used to construct a finite element model. The model error leads to bias in the estimates, and many observations do not eliminate the bias. On the other hand, the measurement error is due to noise effects that contaminate the experimental data. This noise can be induced by electrical devices, problems with cables, etc. This type of error is defined as a random error and produces imprecise measurements, but not bias.

The robustness to model error is here evaluated by modifying the physical and mechanical properties of the FE model, namely the concrete density and the modulus of elasticity of concrete and structural steel. For each method, the number of different sensor positions obtained from the modified FE models, compared to the original FE model, are evaluated as a function of the number of monitored DOFs. This evaluation considers the

parametric uncertainties associated to the discrepancies between the values of the real structure and the input parameters used for the analysis.

Besides, a robustness assessment of the methods to measurement error is carried out by adding a random error to the mode shape displacements obtained with the original FE model. Then, for each method, the number of different sensor positions obtained from the modified mode shape displacements compared to the original FE model are evaluated as a function of the number of monitored DOFs.

The four OSP methods were programmed in MATLAB and the mode shapes obtained from the modal analysis of the FE model were used as input data. Considering that translations in the longitudinal direction (Y-direction) of the footbridge are almost null for the first five mode shapes, only two DOFs per node, corresponding to the vertical translation (Z-direction) and the lateral translation (X-direction), are considered in the analysis. Therefore, assuming that translations are constrained in 14 nodes due to the boundary conditions, 166 DOFs are candidates to be monitored.

The four methods are evaluated in terms of robustness for different numbers of target sensors (ranging from  $N_0 = 5$  to 166). For the identification of the first five modes, the minimum number of sensors is five since it is known that the number of sensors should not be less than the number of mode shapes to be identified [4].

Lizana and Casas [9,10] showed that EFI and IEI methods give the same optimal sensor positions for the range of 5–166 sensors. The optimization of these two methods leads to the largest volume of information and the minimal uncertainty in the system parameters for any number of sensors. Their equivalence in terms of the resulting sensors positions for any number of sensors implies that their optimization criteria are analogous. The MKE method presents the lowest computation time for any total number of sensors, closely followed by the EFI method. It must be remarked that even though the EFI and IEI methods give the same sensor positions, the computation time of the EFI method is significantly lower.

#### 4.1. Robustness to Model Error

The selection of sensor locations is based on the FE model that is likely to contain significant modeling errors compared to the actual bridge. Therefore, the robustness to model error is evaluated by modifying the concrete density and the modulus of elasticity of concrete and structural steel of the FE model. For this purpose, seven FE models were created with modified physical and mechanical properties from the original FE model:

1. Model B1: FE model with an increase of 5% in the Young's modulus of concrete (+5%  $E_c$ )
2. Model B2: FE model with an increase of 10% in the Young's modulus of concrete (+10%  $E_c$ )
3. Model B3: FE model with an increase of 15% in the Young's modulus of concrete (+15%  $E_c$ )
4. Model B4: FE model with an increase of 5% in the Young's modulus of structural steel (+5%  $E_s$ )
5. Model B5: FE model with an increase of 5% in the concrete density (+5%  $\rho_c$ )
6. Model B6: FE model with a decrease of 5% in the concrete density (−5%  $\rho_c$ )
7. Model B7: FE model with an increase of 15% in the Young's modulus of concrete, an increase of 5% in the Young's modulus of structural steel and a decrease of 5% in the concrete density (+15%  $E_c$  + 5%  $E_s$  − 5%  $\rho_c$ )

The physical and mechanical properties used in the seven modified FE models are reported in Table 2. Notation of the locations is shown in Figure 4.



**Table 2.** Modified physical and mechanical properties from original FE model.

Physical and Mechanical Properties	Location	FEM	+5%	+10%	+15%	−5%
$\rho_c$ (kg/m <sup>3</sup> )	P6 & P7	2070.89	2174.43	-	-	1967.35
	P5 & P8	2129.00	2235.45	-	-	2022.55
	P4 & P9	2173.45	2282.12	-	-	2064.78
	P3 & P10	2280.43	2394.45	-	-	2166.41
	Legs	2269.83	2383.32	-	-	2156.34
$E_c$ (GPa)	Mainspan	35.00	36.75	38.50	40.25	-
	Legs	36.00	37.80	39.60	41.40	-
$E_s$ (GPa)	Arch	206.87	217.21	-	-	-
	Pier base	210.64	221.17	-	-	-
	Pier branches	213.04	223.69	-	-	-
	Spandrel	200.36	210.38	-	-	-

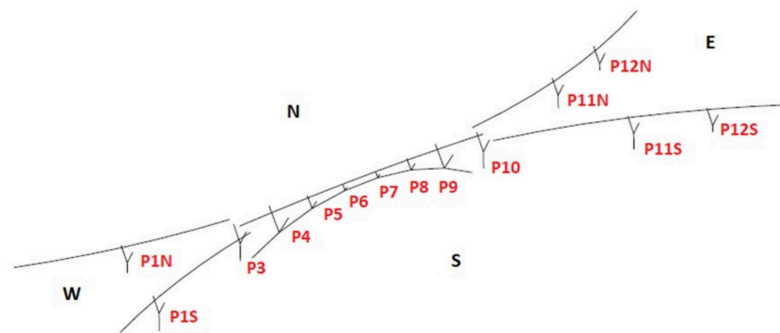


**Figure 4.** Notation of piers and spandrels of the Streicker Bridge.

The following figures represent only the maximum number of different sensor positions among the seven modified FE models for each number of monitored DOFs.

Figure 5 shows the evolution of the number of different sensor positions as a function of the number of monitored DOFs using the MKE method. It can be noticed that in the range of 5–44 sensors and in the range of 112–124 sensors, the number of different sensor positions is zero or one. The effect of the modification of physical and mechanical properties is higher in the range of 92–102 sensors, where five different sensor positions are reached. The analysis present local maxima with comparable peaks (e.g., four different positions are reached for the 66-sensors set).

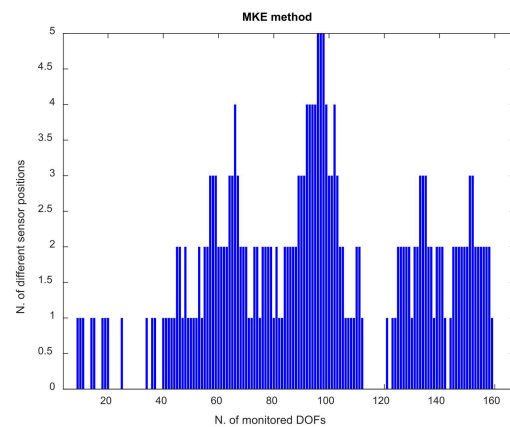


**Figure 5.** Maximum number of different sensor positions obtained from the modified FE models compared to the original FE model as a function of the number of monitored DOFs. MKE method and five mode shapes to be identified.



Figure 6 illustrates the evolution of the number of different sensor positions between the modified FE models and the original FE model using the EFI and IEI methods. It can be observed that in the range of 5–19 sensors and in the range of 37–71 sensors, the number of different sensor positions is zero or one. The effect of the modification of physical and mechanical properties is higher in the range of 114–141 sensors, where six different sensor positions are reached for the 138-sensors set.

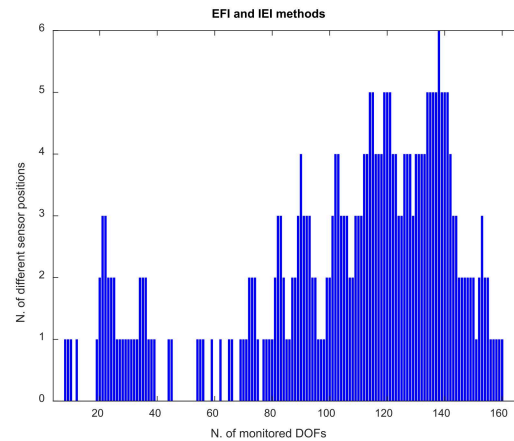


**Figure 6.** Maximum number of different sensor positions obtained from the modified FE models compared to the original FE model as a function of the number of monitored DOFs. EFI and IEI methods and five mode shapes to be identified.

In the range of 5–19 sensors, the MKE, EFI and IEI methods reach a maximum number of different sensor positions of one and then it can be assumed that for practical applications (considering a low number of sensors) the three methods present a similar robustness to the model error. Nevertheless, in the range of 20–40 sensors, the MKE method can be considered more robust to model error since, differently from the EFI and IEI methods, the number of different sensor positions does not exceed one.

Figure 7 shows the evolution of the number of different sensor positions between the modified FE models and the original FE model using the MinMAC method with an initial sensor set formed by a single vertical sensor in node 84. For this method, the number of different positions is much higher compared to the other three methods all over the selecting process. For the 42-sensors set, the number of different sensor positions reaches its maximum with 28 different positions.

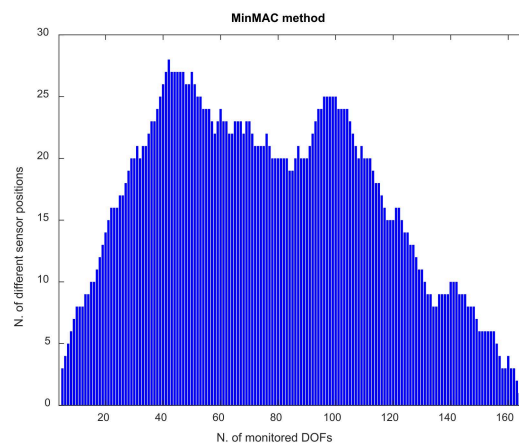


**Figure 7.** Maximum number of different sensor positions obtained from the modified FE models compared to the original FE model as a function of the number of monitored DOFs. MinMAC method and five mode shapes to be identified.

It has been observed that the four OSP methods are more sensible (i.e., less robust) to an increase of 5% in the Young's modulus of concrete (Model B1) than to a variation of 5% in the concrete density (Model B5 and Model B6). In other words, the effect of a biased Young's modulus of the concrete on the optimal sensor configuration is higher than a biased density.

#### 4.2. Robustness to Measurement Error

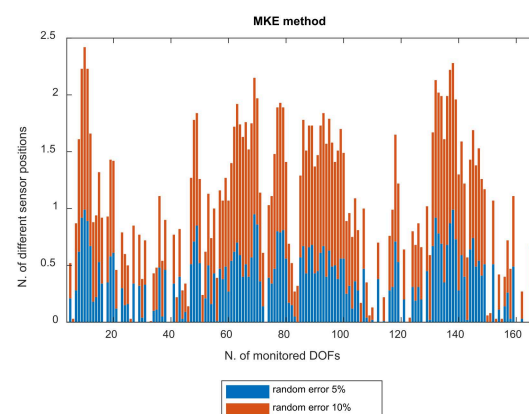
To capture the measurement error due to sensor inaccuracies, a random error is added up to the mode shape displacements of the original FE model. Two different levels of noise are considered: a random error of 5% and of 10%. The levels of noise were simulated as follows: the mode shape displacements of the original FE model were multiplied by a random number between 0.95 and 1.05 for the case of the random error of 5% and by a random number between 0.9 and 1.1 for the case of the random error of 10%.

Considering that displacement transducers (LVDT) give a more accurate measurement of the mode shapes than accelerometers, the random error of 5% could simulate the LVDT error, while the random error of 10% could reproduce the accelerometer error.

The robustness of the four OSP methods (MKE, EFI, IEI and MinMAC methods) to measurement error is evaluated in terms of the number of different sensor positions obtained from the modified mode shape coordinates compared to the original FE model as a function of the number of monitored DOFs.

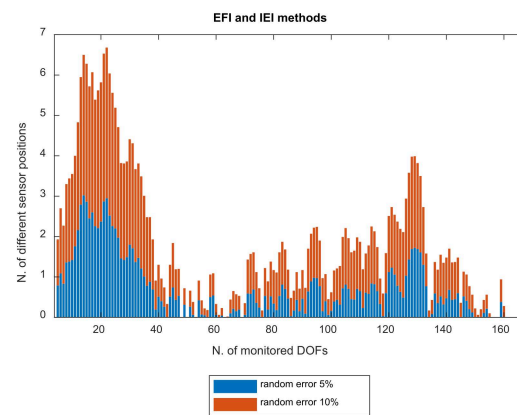
The following figures depict the average number of different sensor positions over 100 measurements as a function of the number of monitored DOFs. Many measurements were performed to capture the robustness to measurement error of the methods, as a few numbers of measurements would emulate the actual experimental campaign, but would not give significant information on robustness. For each method, the number of different positions follows a similar pattern for the two different levels of noise, but it is higher for all cases of total numbers of sensors when the random error of 10% is applied.

Figure 8 shows the average number of different sensor positions over 100 measurements as a function of the number of monitored DOFs using the MKE method. For the 10-sensors set and a random error of 10%, the average number of different sensor positions reaches its maximum with 2.42 different sensors. This value is lower than five, which is the maximum number of different positions due to the model error (see Figure 5 in the range of 92–102 sensors).



**Figure 8.** Average number of different sensor positions over 100 measurements obtained from the modified mode shape displacements compared to the original FE model as a function of the number of monitored DOFs. MKE method and five mode shapes to be identified.

Figure 9 illustrates the average number of different sensor positions over 100 measurements as a function of the number of monitored DOFs using the EFI and IEI methods. For these methods, it can be stated that the effect of the measurement error is more significant for sensor configurations with few sensors, approximately in the range of 5–38 sensors.



**Figure 9.** Average number of different sensor positions over 100 measurements obtained from the modified mode shape displacements compared to the original FE model as a function of the number of monitored DOFs. EFI and IEI methods and five mode shapes to be identified.

The average number of different sensor positions presents a maximum value of 6.68 for the 22-sensors set and a random error of 10%. This value is higher than six, which is the maximum number of different positions due to the model error (see the 138-sensors set in Figure 6).

It can be observed that in the range of 5–38 sensors, the MKE method presents a higher robustness to measurement error than the EFI and IEI methods. Hence, also regarding the measurement error, it can be stated that the MKE method outperforms the EFI and IEI methods in terms of robustness in this initial range of sensors.

Figure 10 shows the average number of different sensor positions over 100 measurements as a function of the number of monitored DOFs using the MinMAC method with an initial sensor set formed by a single vertical sensor in node 84. For this method, the number of different positions is much higher compared to the other three methods all over the selecting process, which means that the MinMAC method is the least robust method to the measurement errors.

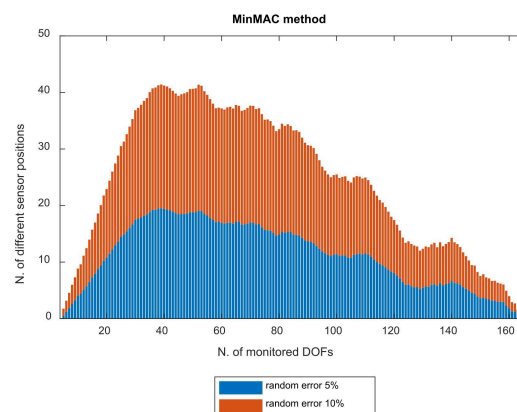


**Figure 10.** Average number of different sensor positions over 100 measurements obtained from the modified mode shape displacements compared to the original FE model as a function of the number of monitored DOFs. MinMAC method and five mode shapes to be identified.

For the 39-sensors set and a random error of 10%, the average number of different sensor positions reaches its maximum with 41.4 different sensors. This value is higher than 28, which is the maximum number of different positions due to the model error (see the 42-sensors set in Figure 7).

## 5. Conclusions

In this paper, four of the most influential OSP methods were evaluated in terms of robustness to model and measurement errors for the identification of the first five mode shapes of a pedestrian bridge. In the range of 5–38 sensors, the MKE method can be considered the most robust method to both model and measurement errors. Conversely, the robustness of the MinMAC method is considerably lower compared to the other three methods all over the selecting process.

According to the results, in a dynamic testing of a pedestrian bridge, the MKE method seems to be the most suitable method to estimate the optimal sensor positions. The MKE method provides a relatively large amount of information with the lowest computational time, and it outperforms the other three methods in terms of robustness in the usual range of number of sensors.

**Author Contributions:** Paper conceptualization due to M.L. and J.R.C. M.L. built the FE model of the footbridge. M.L. programmed the optimal sensor placement analyses in Matlab<sup>TM</sup> and created the figures under the supervision of J.R.C. The final version, prepared by M.L., was obtained after the revision work of J.R.C. All authors have read and agreed to the published version of the manuscript.

**Funding:** This research received no external funding.

**Institutional Review Board Statement:** Not applicable.

**Informed Consent Statement:** Not applicable.

**Data Availability Statement:** The data are contained within the article.

**Acknowledgments:** Branko Glisic is acknowledged to provide technical drawings of the Streicker Bridge. Maria Gabriella Mulas and Marco Domaneschi are acknowledged for their support during M.L. MSc thesis at Politecnico di Milano.

**Conflicts of Interest:** The authors declare no conflict of interest.

## References

1. Giordano, P.F.; Prendergast, L.J.; Limongelli, M.P. Quantifying the value of SHM information for bridges under flood-induced scour. *Struct. Infrastruct. Eng.* **2022**, *1*–17. [[CrossRef](#)]
2. Capellari, G.; Chatzi, E.; Mariani, S. Cost-Benefit Optimization of Structural Health Monitoring Sensor Networks. In Proceedings of the 4th International Electronic Conference on Sensors and Applications, Online. 15–30 November 2017.
3. Castro-Triguero, R.; Murugan, S.; Gallego, R.; Friswell, M.I. Robustness of optimal sensor placement under parametric uncertainty. *Mech. Syst. Signal Process.* **2013**, *41*, 268–287. [[CrossRef](#)]
4. Yi, T.-H.; Li, H.-N. Methodology Developments in Sensor Placement for Health Monitoring of Civil Infrastructures. *Int. J. Distrib. Sens. Netw.* **2012**, *8*, 612726. [[CrossRef](#)]
5. Krammer, D.C. Sensor placement for on-orbit modal identification and correlation of large space structures. *J. Guid. Control Dyn.* **1991**, *14*, 251–259. [[CrossRef](#)]
6. Papadimitriou, C.; Lombaert, G. The effect of prediction error correlation on optimal sensor placement in structural dynamics. *Mech. Syst. Signal Process.* **2012**, *28*, 105–127. [[CrossRef](#)]
7. Carne, T.G.; Dohrmann, C.R. A modal test design strategy for modal correlation. In Proceedings of the 13th International Modal Analysis Conference, Nashville, TN, USA, 13–16 February 1995; pp. 927–933.
8. Lizana, M. Numerical Assessment of the Static and Dynamic Behavior of the Streicker Bridge. Master's Thesis, Politecnico di Milano, Milan, Italy, 2019.
9. Lizana, M.; Casas, J. Optimal sensor placement methods and criteria in dynamic testing—Comparison and implementation on a pedestrian bridge. In Proceedings of the 10th International Conference on Structural Health Monitoring of Intelligent Infrastructure (SHMII 10), Porto, Portugal, 30 June–2 July 2021.
10. Lizana, M. Optimal Sensor Placement Methods and Criteria in Dynamic Testing. Comparison and Implementation on a Pedestrian Bridge. Master's Thesis, Universitat Politècnica de Catalunya, Barcelona, Spain, 2020.